06;13

Angular dependence peculiarities of germanium sputtering yield with a focused gallium ion beam

© M.A. Smirnova[1,2], K.N. Lobzov[1,2], V.I. Bachurin[2], L.A. Mazaletsky[1,2], D.E. Pukhov[2], A.B. Churilov[2]

[1] Demidov State University, Yaroslavl, Russia
[2] Valiev Institute of Physics and Technology of RAS, Yaroslavl Branch, Yaroslavl, Russia
E-mail: vibachurin@mail.ru

Received April 26, 2024
Revised June 28, 2024
Accepted July 18, 2024

Angular dependences of Ge and Si sputtering yields with a 30 keV focused Ga^+ ion beam are reported. Comparison between experimental angular dependence of Ge sputtering yield and corresponding SDTrimSP simulation data reveals considerable differences. Thus, the experimental data exceed the simulation data at incidence angles from 0° to 50° and at larger angles they have a lower value, whereas for Si these dependences are in good agreement. The angular dependence peculiarities of Ge sputtering yield are attributed to the development and change of the surface topography at oblique ion incidence.

Keywords: germanium, ion bombardment, sputtering yield, surface topography.

DOI: 10.61011/TPL.2024.11.59672.19975

Focused ion beams (FIB) are used widely to form nanostructures on the surface of various materials. Before carrying out experiments using FIB facilities are normally preceded by modeling [1] that requires data on angular dependences.

To date, there are few reports devoted to the angular dependences of silicon [2] and SiO2 [3] sputtering using Ga^+ FIBs. In the present study, the results of measurements of the angular dependence of germanium sputtering yield $Y(\theta)$ in experiments with Ga^+ FIBs with an energy of 30 keV at angles of ion baem incidence ranging from 0 to 85° are reported. An experimental $Y(\theta)$ dependence for Si within the specified angular range and $Y(\theta)$ dependences for Ge and Si calculated in the SDTrimSP program were also obtained for comparison. Germanium was chosen as an investigation object due to the wide application of this material in microelectronic technologies. Specifically, Ge is used as anode material in lithium-ion batteries [4]. At the same time, it is known that irradiation of Ge with ions of various gases and metals leads to the formation of a porous surface structure [5–8]. It was demonstrated in [9] that such a structure forms when Ge is irradiated with a focused beam of Ga^+ ions with an energy of 30 keV and fluence $D = 5 \cdot 10^{15} - 10^{16}\,\mathrm{cm}^{-2}$. Meanwhile, the modified layer thickness is ~ 90 nm, and the pore diameter increases from 20 to 50 nm, respectively. A sponge-like structure forms at higher fluences. The porous layer thickness increases to 150 nm in this case, the pore diameter is ~ 80 nm, and the thickness of walls between pores remains unchanged (~ 20 nm). In experiments with oblique ion incidence, the pores are tilted in concert with the trajectory of ions. It is known that the surface relief has a strong influence on the average value of Y [10]. It was demonstrated in [11] that the value of Y obtained by molecular dynamics modeling of the process of sputtering of Au nanocrystals by Ga^+ ions with an energy of 25 keV is significantly higher than the one corresponding to sputtering of bulk material. It was established by secondary ion mass-spectrometry that the mass spectrum of porous Si differs from the spectrum of bulk Si in having a higher yield of cluster secondary ions [12]. The maximum yield of such ions is characteristic of structures with the smallest size of pore walls. The authors attributed this fact to the possibility of yielding of the maximum number of sputtered particles. It is reasonable to expect that the topography of the Ge surface [9], which varies with ion incidence angle, should affect the angular dependence of $Y(\theta)$ of germanium, the determination of which was the goal of the present study.

Experiments on the measurement of sputtering yields of Si (100) and Ge (110) with Ga^+ ions with an energy of 30 keV were carried out using a Quanta 3D 200i facility. The beam diameter was 60 nm, the current was 3 nA, incidence angle θ varied from 0 to 85° relative to the surface normal, and $D = 5 \cdot 10^{17}\,\mathrm{cm}^{-2}$. Rasters patterns $30 \times 13\,\mu$m in size were formed on the surface. The geometric dimensions of sputtering craters were determined with a SUPRA 40 scanning electron microscope (SEM). These data were used to calculate the volume and mass of sputtered material [2]. In the case of Ge sputtering, the depth of craters was an order of magnitude greater than the thickness of the modified layer. Irradiation experiments were carried out at $T = 300$ K. The angular dependences of Si and Ge sputtering yields with Ga^+ ions with an energy of 30 keV and the parameters of atomic collision cascades initiated by ion bombardment were calculated using SDTrimSP. The surface topography of irradiated samples was also investigated by SEM. Cross-sections of samples (along the beam propagation direction) obtained

by irradiating Ge with Ga^+ ions were prepared *in situ* at the Quanta 3D 200i facility. Subsequent SEM analysis was carried out *ex situ*.

Figure 1 presents the angular dependences of sputtering yields of Si (a) and Ge (b) obtained experimentally and using SDTrimSP modeling; the $Y(\theta) = Y(0)\cos^{-2}\theta$ Sigmund model approximation is also shown. It follows from Fig. 1, a that the experimental data for Si samples agree closely with the calculated ones. In contrast, the experimental data for germanium sputtering by a Ga^+ FIB differ significantly from the results of modeling, which normally provides a fine fit to experiments and approximations. The experimental values of the sputtering yield remain higher than the calculated ones at incidence angles $\theta \leqslant 50^\circ$ (at angles close to the normal, the difference is almost 1.5-fold); at larger incidence angles, the experimental yield is lower. It can also be seen that the sputtering yield increases by a factor of 1.5–2 at the most, while a 4–6-fold enhancement is observed for Si and other single-element materials. Under normal incidence of a Ga^+ ion beam, $Y(0) = 6.2 \pm 0.5$ atoms/ion for Ge. This

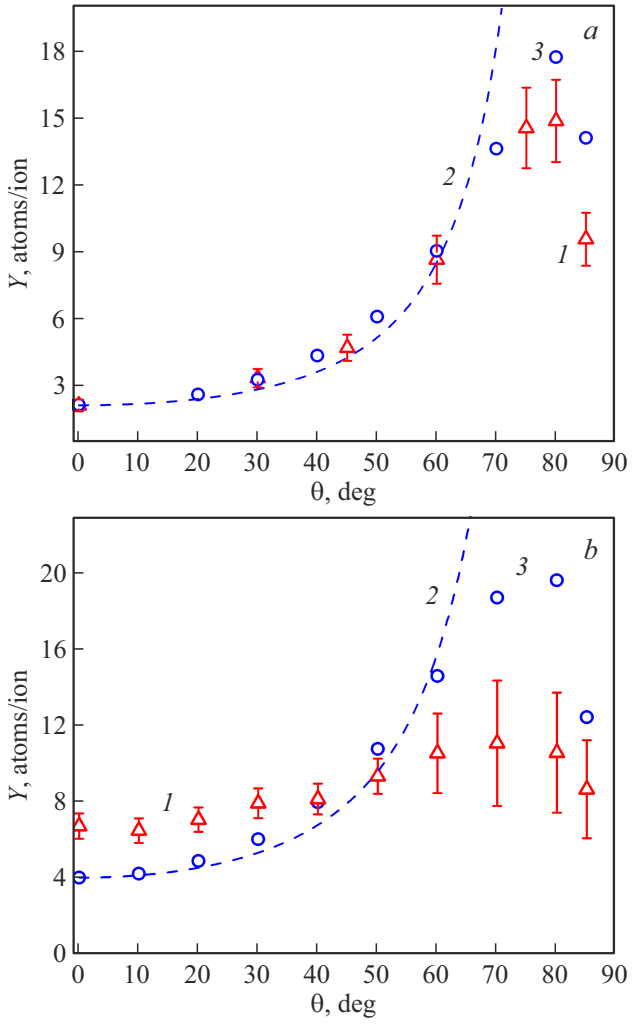

Figure 1. Angular dependences of silicon (a) and germanium (b) sputtering yield. *1* — Experimental data; *2* — $Y(\theta) = Y(0)\cos^{-2}\theta$ approximation; *3* — results of simulation in SDTrimSP.

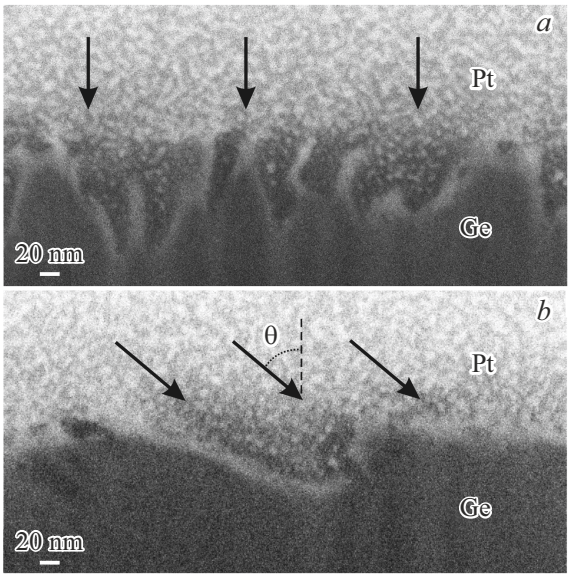

Figure 2. Electron-microscopic images of cross-sections of sputterig crsters formed under normal (a) and oblique (b) irradiation with Ga^+ ions: $\theta = 0$ and 50°, respectively. $D = 5 \cdot 10^{17}\,\mathrm{cm}^{-2}$. The direction of ion beam incidence is indicated by arrows.

value matches almost perfectly the one reported in [13] for Ge sputtering by Ge^+ ions with an energy of 30 keV. Since the masses of Ga and Ge ions are close, it can be said that the obtained experimental data on the angular dependence of the sputtering yield of Ge are reliable. Their deviation from the results of modeling may be attributed to the specifics of Ge surface topography forming as a result of ion bombardment at different beam incidence angles.

When sputtering is simulated in SDTrimSP, the sample surface remains flat. As was noted above, a porous structure forms in the near-surface layer at fluences above $D = 5 \cdot 10^{15}\,\mathrm{cm}^{-2}$. As the fluences increase, it transforms (under normal ion incidence) into a sponge-like morphology, which changes in the case of oblique incidence of an ion beam [9]. Figures 2 and 3 show the SEM-images of sputtering craters cross-sections obtained at fixed $D = 5 \cdot 10^{17}\,\mathrm{cm}^{-2}$ and $\theta = 0$, 50° (Fig. 2), 70, and 80° (Fig. 3). It is evident that the local angle of ion incidence onto the top, bottom, and walls of pores may vary from 0 to 90° under normal beam incidence onto a flat surface. This is one of the reasons for the observed increase in sputtering yield. As was noted above, the thickness of walls of the porous structure is ~ 20 nm. This is comparable to the average depth of the energy distribution function of Ga ions in Ge relative to the surface (the projected ion average range a) and its width along the axes parallel and perpendicular to the direction of ion incidence (longitudinal (α) and transverse (β) straggling). The modeling results for sputtering of spherical Si samples with radius R by Ar^+ ions with an energy of 20 keV were presented in [14]. It was found that, under the $a \propto R$ condition, the sputtering yield for spherical samples is almost 3 times higher than the

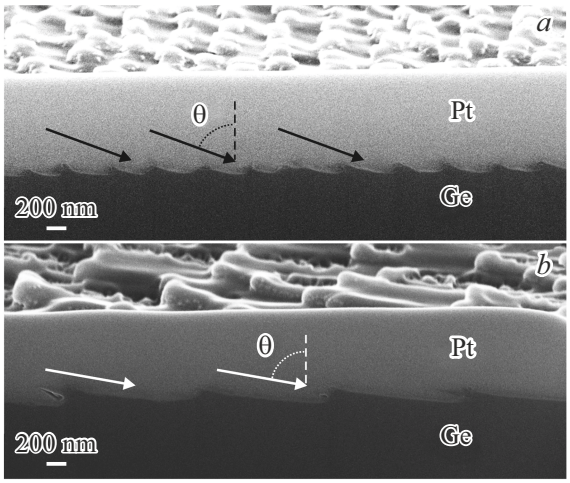

Figure 3. Electron-microscopic images of cross-sections of sputterig crsters formed at near-grazing angles of incidence of Ga^+ ions: $\theta = 70$ (a) and 80° (b). $D = 5 \cdot 10^{17}$ cm^{-2}. The direction of ion beam incidence is indicated by arrows.

corresponding yield for flat ones. This effect is attributable to the fact that the region of deposited energy occupies almost the entire volume of the sphere, and the increase in sputtering is supported by the mechanism of thermal peaks. Therefore, the activation of sputtering mechanisms differing from the linear Sigmund model may also contribute to the enhancement of sputtering yield relative to the modeling data at incidence angles close to the normal.

A wave-like relief forms on the surface (Figs. 2, b and 3) at $\theta \geqslant 50°$. According to SEM data, the local angles of ion incidence onto the front and back slopes of waves are close to 0° and higher than 80°, respectively. This may reduce the average sputtering yield for a surface with a developed relief compared to that for a smooth surface at $\theta \geqslant 50°$.

Thus, experimental and simulated (in the SDTrimSP program) data on the angular dependences of the sputtering yields of silicon and germanium with a Ga^+ FIB with an energy of 30 keV were presented. It was found that experimental dependence $Y(\theta)$ for germanium differs from the calculated one, while similar results for Si samples agree fairly closely. The peculiarities of $Y(\theta)$ for germanium are attributable to the evolution and variation of the surface topography under normal and oblique ion irradiation.

Funding

This work was carried out with financial support from the Ministry of Education and Science of the Russian Federation within the framework of the state assignment of P.G. Demidov Yaroslavl State University No. FENZ-2024-0005, using the equipment of the Facilities Sharing Center „Micro- and nanostructures diagnostic“.

Conflict of interest

The authors declare that they have no conflict of interest.

References

[1] N.I. Borgardt, R.L. Volkov, A.V. Rumyantsev, Yu.A. Chaplygin, Tech. Phys. Lett., **41** (6), 610 (2015). DOI: 10.1134/S106378501506019X.
[2] V.I. Bachurin, I.V. Zhuravlev, D.E. Pukhov, A.S. Rudy, S.G. Simakin, M.A. Smirnova, A.B. Churilov, J. Surf. Investig., **14** (4), 784 (2020). DOI: 10.1134/S1027451020040229.
[3] A.V. Rumyantsev, N.I. Borgardt, R.L. Volkov, Yu.A. Chaplygin, Vacuum, **202**, 111128 (2022). DOI: 10.1016/j.vacuum.2022.111128
[4] N.G. Rudawski, B.L. Darby, B.R. Yates, K.S. Jones, R.G. Elliman, A.A. Volinsky, Appl. Phys. Lett., **100** (8), 083111 (2012). DOI: 10.1063/1.3689781
[5] D.J. Erb, D.A. Pearson, T. Škereň, M. Engler, R.M. Bradley, S. Fasco, Phys. Rev. B, **109** (4), 045439 (2024). DOI: 10.1103/PhysRevB.109.045439
[6] T.P. Gavrilova, V.F. Valeev, V.I. Nuzhdin, A.M. Rogov, D.A. Konovalov, S.M. Khantimerov, A.L. Stepanov, Tech. Phys., **69** (4), 578 (2024). DOI: 10.61011/JTF.2024.04.57532.276-23.
[7] N. Oishi, F. Koga, N. Nitta, Vacuum, **213**, 112123 (2023). DOI: 10.1016/j.vacuum.2023.112123
[8] N. Oishi, N. Higashide, N. Nitta, J. Appl. Phys., **135** (14), 144301 (2024). DOI: 10.1063/5.0199118
[9] M.A. Smirnova, V.I. Bachurin, D.E. Pukhov, L.A. Mazaletsky, M.E. Lebedev, A.B. Churilov, St. Petersburg Polytech. Univ. J. Physics and Mathematics, **16** (3.1), 21 (2023). DOI: 10.18721/JPM.163.103
[10] U. Littmark, W. Hoffer, J. Mater. Sci., **13** (12), 2577 (1978). DOI: 10.1007/BF00552687
[11] T.T. Järvi, K. Nordlund, Nucl. Instrum. Meth. Phys. Res. B, **272**, 66 (2012). DOI: 10.1016/j.nimb.2011.01.034
[12] A.E. Ieshkin, A.B. Tolstoguzov, S.E. Svyakhovskiy, M.N. Drozdov, V.O. Pelenovich, Tech. Phys. Lett., **45** (1), 37 (2019). DOI: 10.1134/S1063785019010267.
[13] Y. Yamamura, H. Tawara, Atom. Data Nucl. Data Tabl., **62** (2), 149 (1996). DOI: 10.1006/adnd.1996.0005
[14] M.L. Nitiadi, L. Sandoval, H.M. Urbassek, W. Möller, Phys. Rev. B, **90** (4), 045417 (2014). DOI: 10.1103/PhysRevB.90.045417

Translated by D.Safin